

AD-A108 519

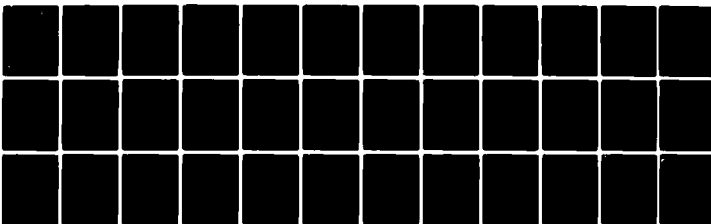
WISCONSIN UNIV-MADISON DEPT OF CHEMICAL ENGINEERING  
PROPERTIES OF MULTIPHASE POLYURETHANE SYSTEMS.(U)  
AUG 81 S L COOPER

F/G 11/9

N00019-80-C-0367

ML

UNCLASSIFIED

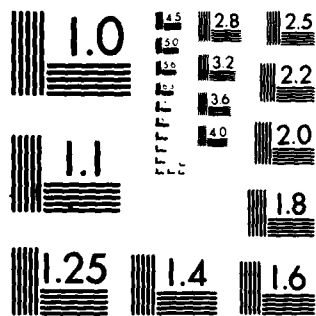


END

DATE

FILED

DTIC



MICROCOPY RESOLUTION TEST CHART  
NATIONAL BUREAU OF STANDARDS-1963-A

AD A108519

LEVEL

6

FINAL REPORT FOR THE PERIOD JULY 1, 1980-JUNE 30, 1981

NAVAL AIR SYSTEMS COMMAND CODE 5163 D2

NAVY CONTRACT # N 00019-80-C-0367

DTIC  
ELECTE  
DEC 1 0 1981

H

STUART L. COOPER  
DEPT. OF CHEMICAL ENGINEERING  
UNIVERSITY OF WISCONSIN  
MADISON, WI 53706

AUGUST, 1981

DTIC FILE COPY

[Approved for public release; distribution unlimited]

81 12 08 066

## PROPERTIES OF MULTIPHASE POLYURETHANE SYSTEMS

FINAL REPORT July 1, 1980-June 30, 1981

### I. POLYURETHANE BLENDS

#### A. INTRODUCTION

→ The objective of this research was to explore the influence of morphology on the structure-property relationships of polyvinylchloride-polyurethane blend systems. →

ET-38-1 is a polyether based polyurethane containing 38 wt% MDI. The molar ratios of the polymer are 3:2:1 (MDI: butane diol: 1000 mw polytetrahydrofuran). The sample compositions were identified as (wt% of ET-38-1)/(wt% of PVC). In order to investigate how the morphological structure affects the material properties, the samples were prepared by three methods: (1) Films were spin cast from a solution of the polymers dissolved in tetrahydrofuran (THF), (2) Films were spin cast from a solution of the polymers dissolved in a solvent mixture of THF and p-dioxane and (3) spin cast films were prepared in the same way as series 1 and were then melt processed by compression molding. The sample preparation method has been found to be very critical in governing the blend's morphology. For example, THF-dioxane solution casting and melt processing produced an incompatible blend while the same materials were made kinetically compatible by precipitation from THF solutions. The compatible polyurethane-PVC system contains a well-mixed PVC-polyether matrix phase as evidenced by  $T_g$  shifts, orientation characteristics, and infrared peak position changes. The aromatic urethane segments which exhibit microphase separation in

the pure polyurethane are not solubilized by blending with PVC by any of sample preparation methods used in this study.

## B. RESULTS AND DISCUSSION

Studies on blends of a segmented polyether polyurethane ET-38-1 with PVC were carried out utilizing differential scanning calorimetry (DSC), Rheovibron, stress-strain, infrared peak positions studies, and infrared dichroism experiments.

### Thermal Analysis

The thermal properties of the ET-38-1/PVC blends were characterized by DSC. For series 1 blends, a heat thermogram was taken respectively on the samples as prepared and after the sample had been slowly cooled from the molten state. A comparison of the two curves illustrates that in the first run the glass transition region of polytetramethylene oxide (PTMO, the soft segment of ET-38-1) is broader and the  $T_g$  (Table 1) is higher than that observed in the second run. In the first run the glass transition of PVC is either not discernible or at a lower temperature than in the second run. In the second run, there are two distinct  $T_g$ 's, each of which corresponds to one of the constituent components.

Series 2 blends are incompatible as evidenced by the observation of two separate  $T_g$ 's originating from each blend component. Similar behavior is observed also in the compression molded samples (series 3).

The results of thermal analysis indicate that by applying different sample preparation methods, one obtains a partially compatible system in series 1 and an incompatible blend in both

Accession For  
NTIS CRIST  
DTIC I-3  
Unannounced  
Jurnal 1981

5

5

5

5

chemical groups on the dissimilar polymer segments, this may induce compatibility due to a favorable exothermic heat of mixing. If interactions between functional groups occurs, the peak position of the participating groups should shift to reflect this. In an incompatible blend system, on the other hand, one would expect only a weighted superposition of the spectra of the constituent components. Peak positions do not shift in an incompatible system because the segmental environment is unaffected by blending. We have investigated the IR peak position shifts of certain functional groups in order to search for specific molecular interactions in series 1 and 2 samples. The  $\text{NH}_\text{B}$  (or  $\text{CO}_\text{B}$ ) peaks as a function of blend composition stay within a range of  $1 \text{ cm}^{-1}$ . This indicates urethane hard segment phase separation in blends of series 1 and 2. However, the  $\text{CO}_\text{F}$  in series 1 samples shows a significant shifting to lower frequency with increasing PVC concentration compared to the blends of series 2 whose  $\text{CO}_\text{F}$  remains unchanged. The series 1  $\text{CO}_\text{F}$  groups appear to be influenced by the  $\alpha$ -hydrogen on the PVC in the compatible PTMO-PVC system.

#### Dynamic Mechanical Properties

Dynamic mechanical measurements using the rheovibron have been applied to ET-38-1/PVC blends of series 1, 2, and 3. In series 1 blends, the appearance of a single  $T_g$  suggests phase mixing of PTMO (soft segment of ET-38-1) with PVC. The increase in  $T_g$  is due to an increase in the relative PVC content of the amorphous PTMO-PVC phase. The observed change in the local mode motion ( $-25^\circ\text{C}$  peak) of PVC also indicates that the segmental

environment of PVC has been altered by intimate mixing with PTMO.

The data for both series 2 and 3 blends show two  $T_g$ 's at  $-10^\circ\text{C}$  ( $\alpha_1$ ) and  $100^\circ\text{C}$  ( $\alpha_2$ ) which are due to the backbone motion of PTMO and PVC, respectively. Since each phase is pure enough to exhibit its own  $T_g$ , series 2 and 3 samples are considered to be incompatible ET-38-1/PVC blends.

Despite the observed difference between blends of series 1 and series 2 or 3, MDI-BD (hard segment of ET-38-1) forms a distinct phase in all three series of blend systems and acts as a filler of high modulus leading to good mechanical properties.

#### Tensile Properties

Uniaxial stress-strain experiments were made on all three series of blends using an Instron tensile tester at room temperature. Only the stress-strain curves for series 1 blends are shown here (Figure 2), since both series 2 and 3 samples show very similar responses. All stress-strain data are summarized in Table 2.

For the three series of polyurethane blends, an increase in the PVC content generally reduced the elongation at failure and greatly increased the Young's modulus. PVC appears to act as an effective "stiffening agent" for polyurethane in these blends. Although blends of series 2 and 3 are incompatible, based on the results from DSC and Rheovibron, there must exist substantial interaction of the two blending components (such as effective interfacial bonding) since rather good mechanical properties are obtained. Thus, the blends of series 2 and 3 can be called mechanically compatible, since their mechanical



properties are enhanced over those which would be obtained from a truly incompatible system.

Since the stress-strain testing was done at room temperature, the results depend strongly upon the viscoelastic state of the specimens. The dynamic mechanical data indicate that, at room temperature, series 1 samples are near  $T_g$  in the leathery region, while series 2 and 3 are both in the rubbery state if only the continuous PTMO phase is considered. Because PVC has a higher  $T_g$  than PTMO, the partially compatible blends (series 1) are stiffer than the incompatible samples (series 2 and 3). This is verified by comparing the Young's moduli for blends of the same compositions.

#### Morphological Models

A morphological model of series 1 blends is shown in Figure 3. The heavy lines represent polyurethane hard segments which aggregate into hard domains. Shorter hard segments may be dispersed in the matrix phase which is a compatible PTMO-PVC mixture.

Figure 4 shows a model for series 2 and 3 blends of ET-38-1/PVC. The MDI-BD domains still have the same morphology as in the series 1 samples but are not visible at the scale of this representation. The PVC domains exist either as an inclusion or as an interconnecting network depending on PVC concentration.

#### C. SIGNIFICANCE

As determined from DSC and Rheovibron data, THF-dioxane solution casting and melt processed samples are incompatible

while THF solution casting produced a partially compatible polyurethane-PVC blend. However, similar uniaxial stress-strain data on all three series of samples indicate substantial polyether (soft segment of polyurethane) plasticization effect upon PVC, and therefore all of the blends can be considered as mechanically compatible. This produces useful blend systems of satisfactory mechanical properties with the PVC acting as a polyurethane stiffening agent. Such blends also exhibit improved flammability characteristics which are inherent to the PVC component. This is especially valuable in foamed elastomer or plastic applications.

TABLE 1

GLASS TRANSITION TEMPERATURES OF ET-38-1/PVC BLENDS  
(DSC DATA) °C

<u>ET-38-1/PVC</u>	<u>FIRST</u>	<u>SECOND</u>	<u>QUENCH</u>
SERIES ONE			
100/0	-41	-32, -	-10, -
90/10	-39	-30, -	-9, -
75/25	-29	-31, 81	-12, 83
62.5/37.5	-31	-34, 81	-11, 83
50/50	-	-31, 81	-11, 82
37.5/62.5	-	-34, 82	-16, 83
25/75	80	-41, 79	-19, 83
10/90	68	- , 79	- , 81
0/100	59	- , 75	- , 78
SERIES TWO			
100/0	-41, -		
75/25	-40, 92		
62.5/37.5	-35, 91		
50/50	-34, 92		
37.5/62.5	-32, 89		
25/75	-41, 90		
0/100	- , 87		
SERIES THREE			
75/25	-39, 83		
62.5/37.5	-42, 82		
50/50	-41, 80		
37.5/62.5	-48, 82		
25/75	-47, 80		

TABLE 2

## TENSILE PROPERTIES OF ET-38-1/PVC BLENDS

ET-38-1/PVC	ELONGATION AT FAILURE %	ULTIMATE TENSILE STRENGTH ( $10^7$ Newton/m <sup>2</sup> )	YOUNG'S MODULUS ( $10^7$ Newton/m <sup>2</sup> )
SERIES ONE			
100/0	505	5.26	3.54
90/10	484	5.09	4.55
75/25	370	4.44	12.57
62.5/37.5	318	4.20	28.54
50/50	237	3.41	68.36
37.5/62.5	218	3.98	134.48
25/75	-	3.7*	207
10/90	-	4.2*	301
0/100	2	5.95	371
SERIES TWO			
100/0	614	3.37	4.82
75/25	385	2.8	13.20
62.5/37.5	310	2.74	20.05
50/50	378	4.15	38.27
37.5/62.5	316	4.09	89.08
25/75	-	3.2*	74.71
0/100	-	-	262
SERIES THREE			
100/0	579	4.8	4.91
75/25	411	3.26	14.64
62.5/37.5	316	3.36	27.58
50/50	198	2.52	68.19
37.5/62.5	189	3.10	114
25/75	155	3.77	168
10/90	-	3.5*	270
0/100	-	4.7*	336

\* : ESTIMATED VALUE.

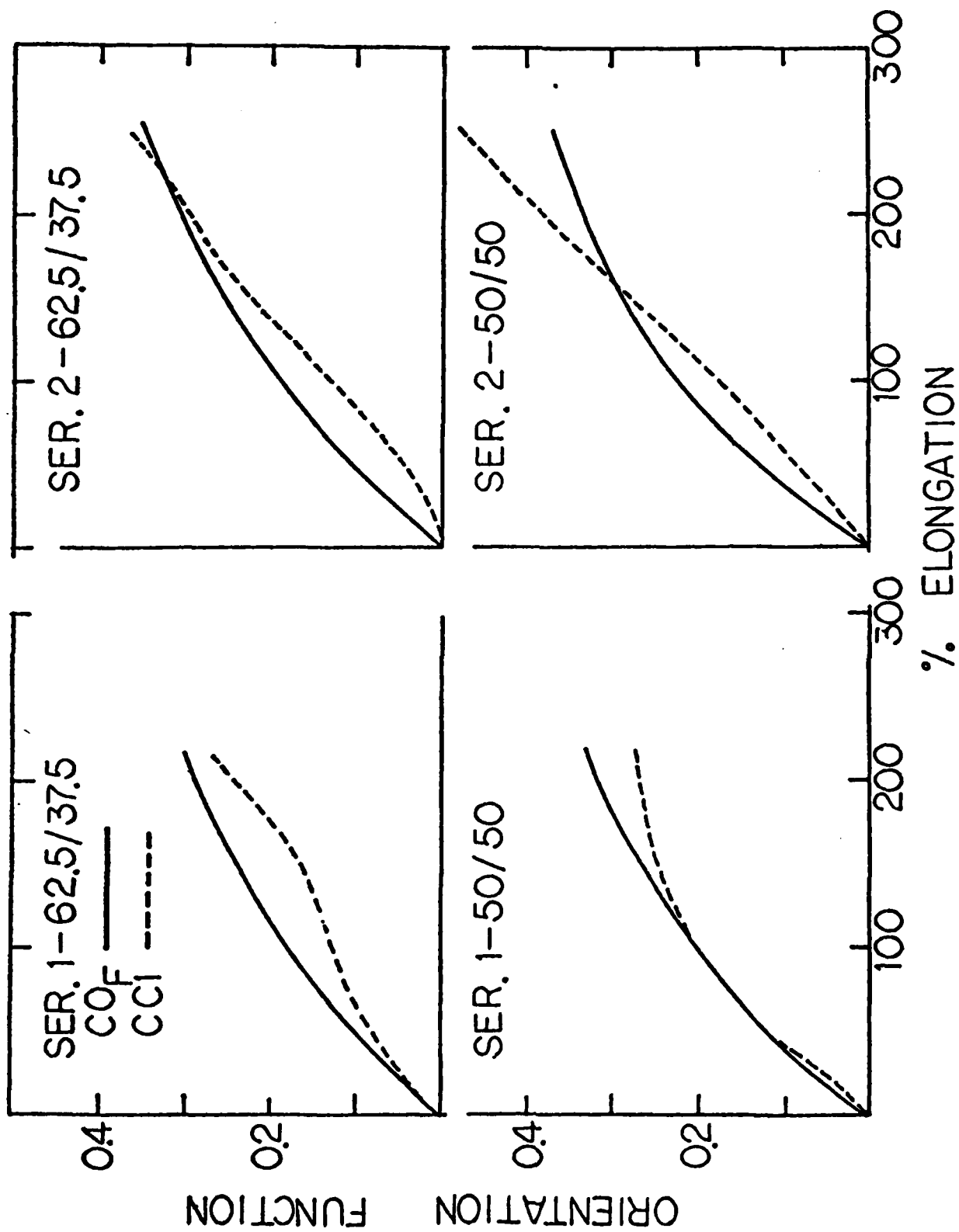


FIG. 1

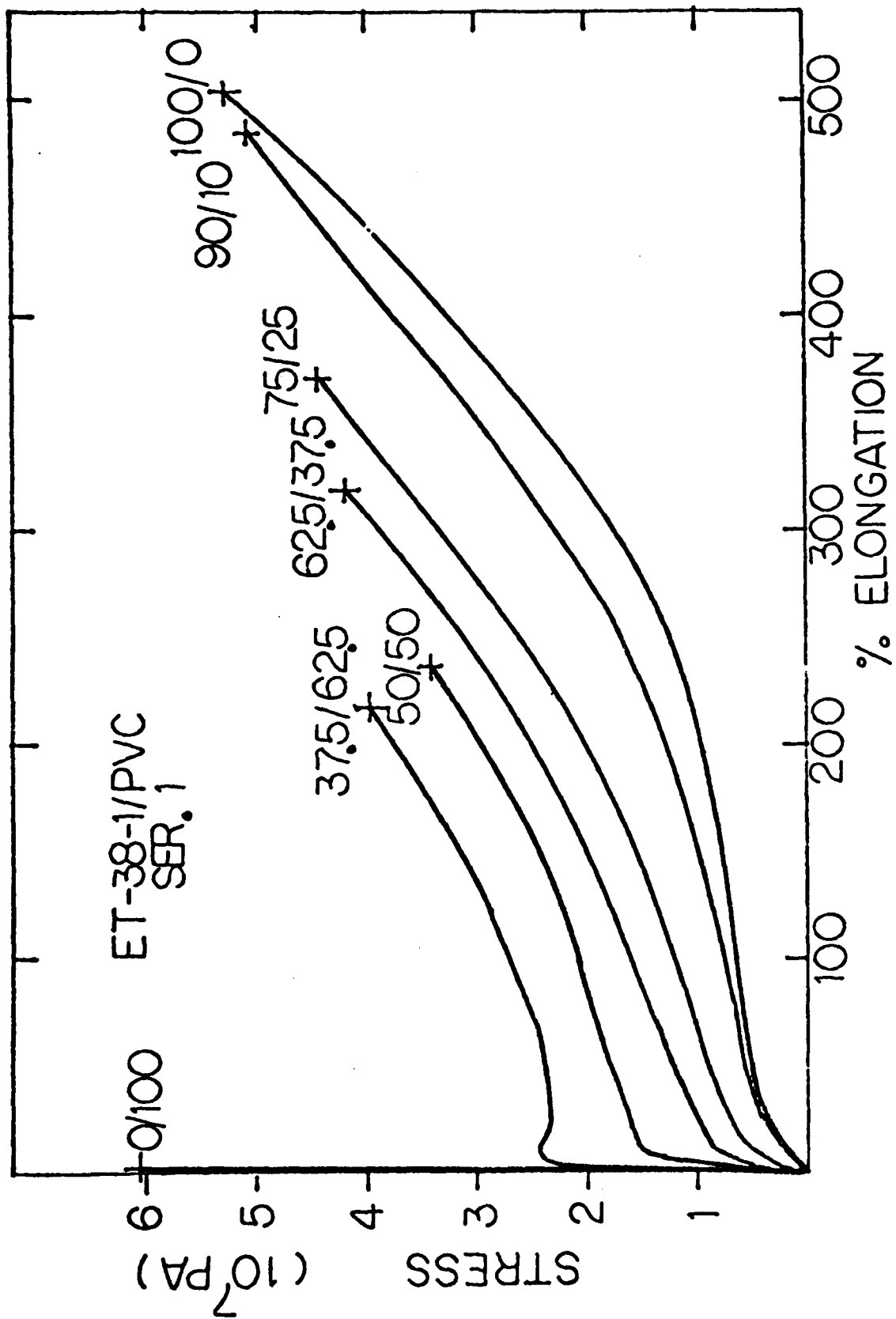
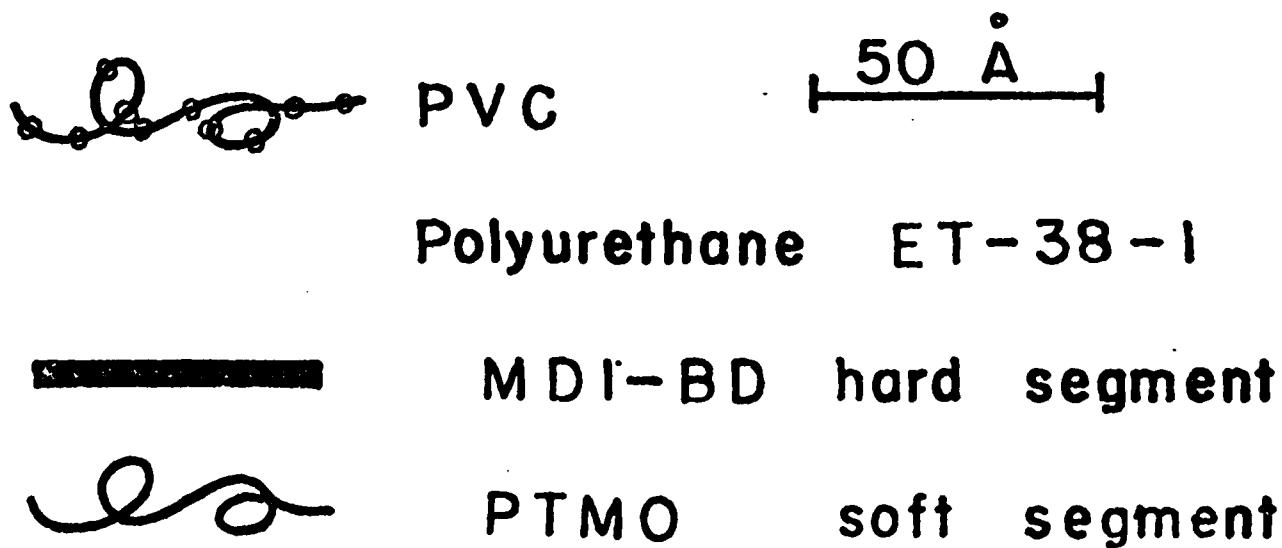
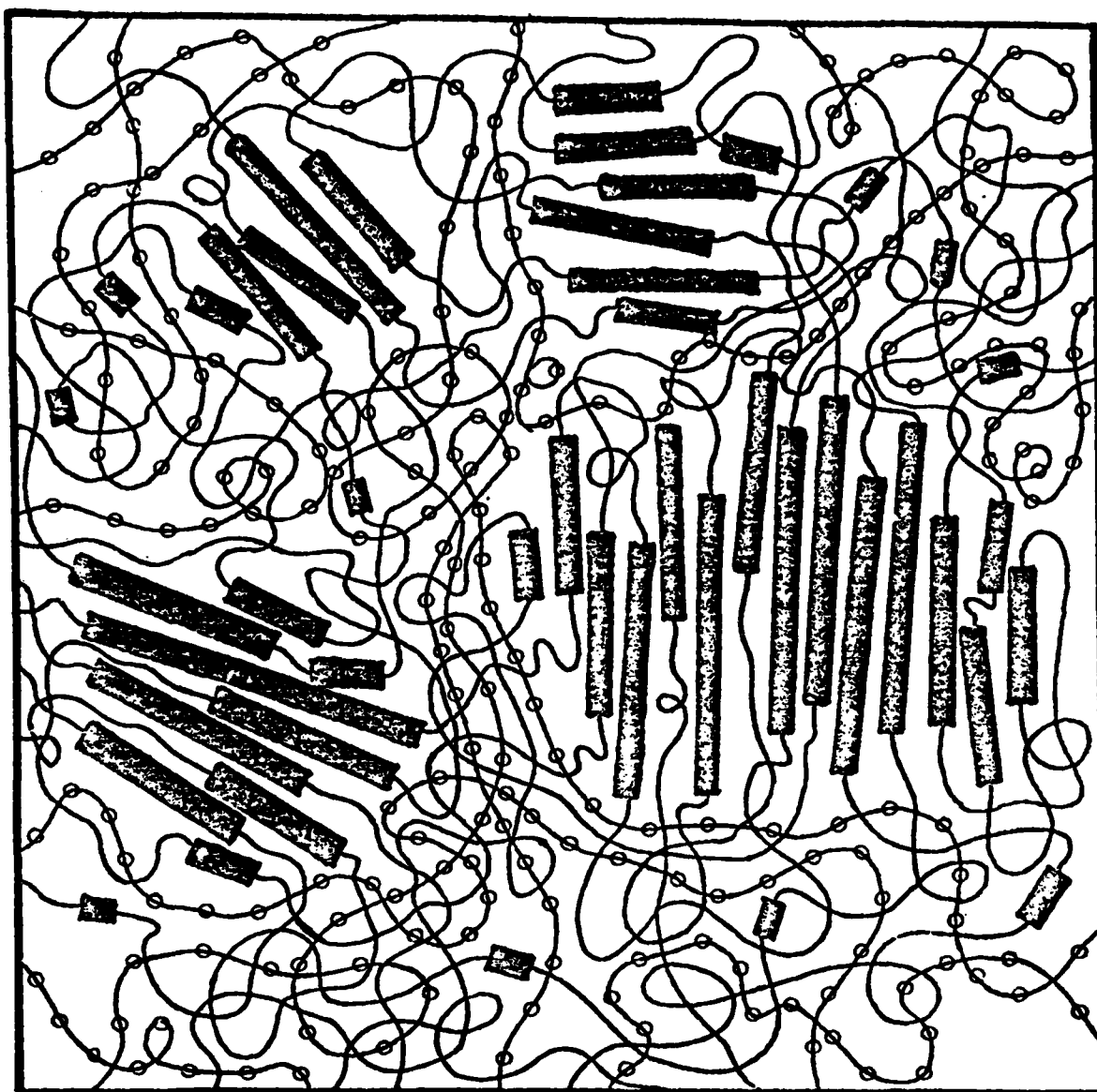
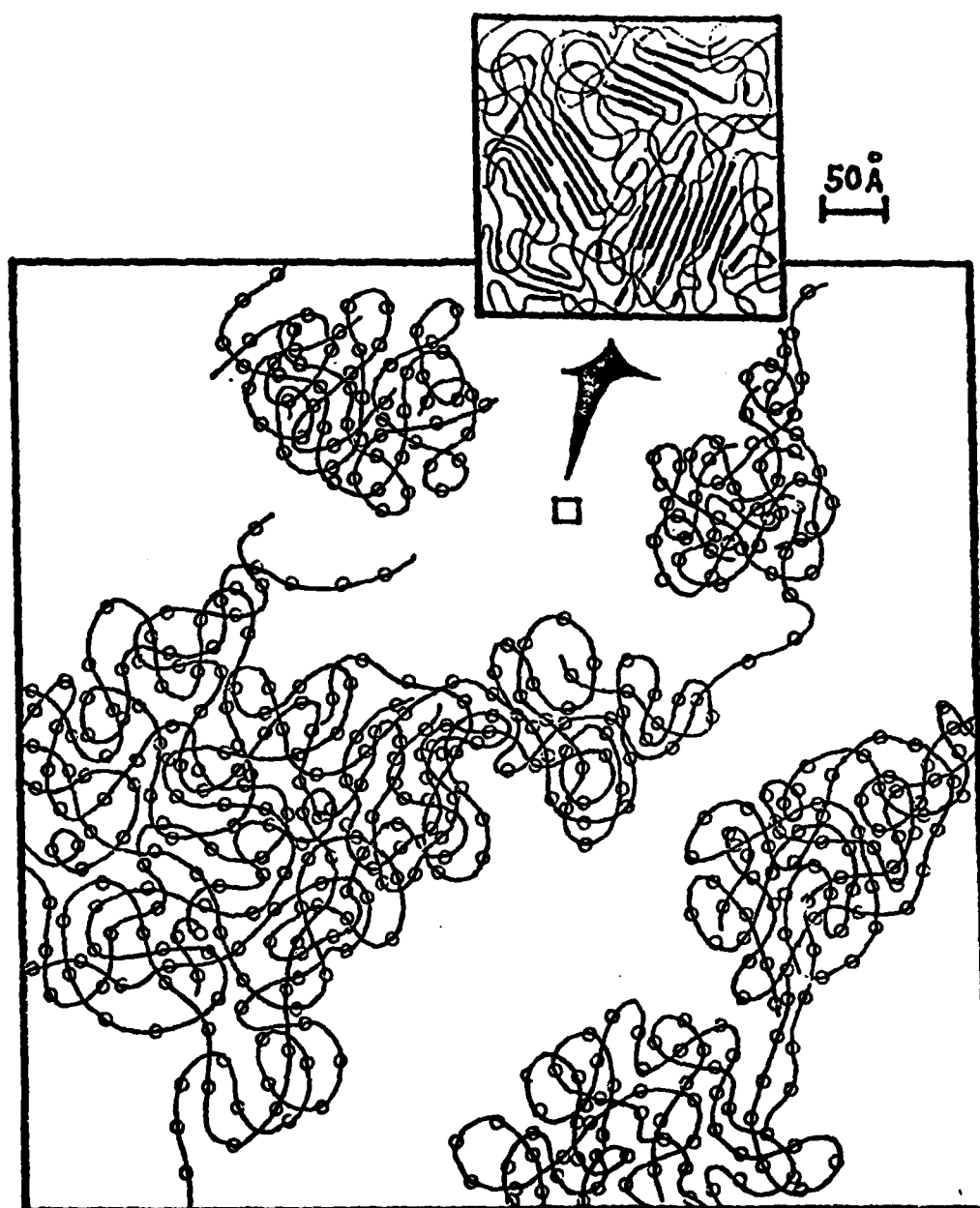


FIG. 2






PVC

1 μ

OPEN AREA

Polyurethane ET-38-1

1.  MDI-BD hard segment

2.  PTMO soft segment

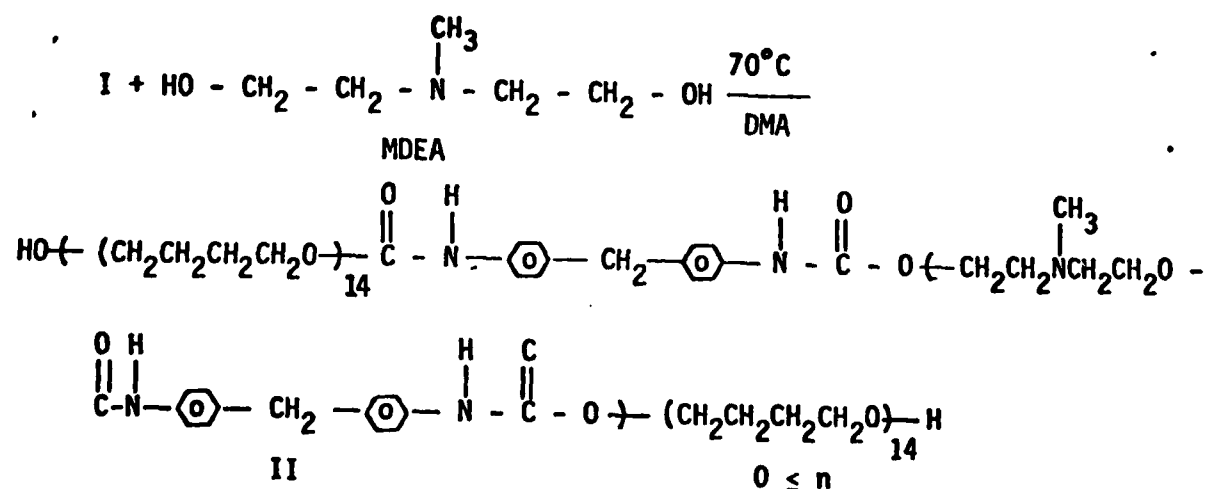
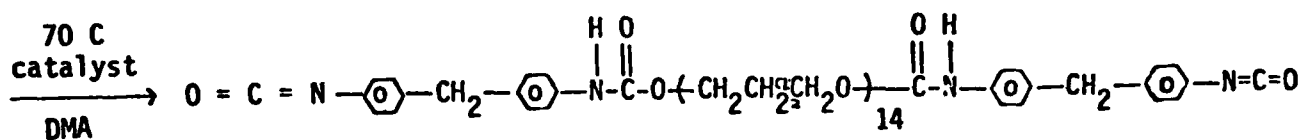
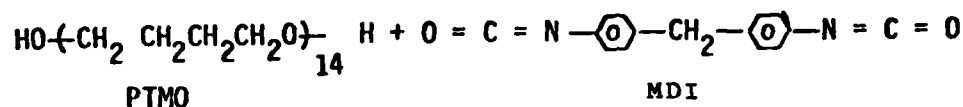


## II. POLYURETHANE IONOMERS

### A. INTRODUCTION

During the past year, two families of polyurethane ionomers were synthesized (zwitterionomers and anionomers). The zwitterionomers were based on 4,4'-diphenylmethane diisocyanate (MDI), N-methyl diethanolamine (MDEA) and polytetramethylene oxide (PTMO) and were synthesized with four levels of hard segment content (Scheme I). The tertiary amine of MDEA of each of these polymers subsequently reacted with  $\gamma$ -propane sultone producing several levels of ammonium sulfonation (Scheme II)

#### MDI/MDEA/PTMO Series



Scheme I. Synthesis of Segmented Polyether Polyurethane.



the anion as well.

$$\begin{array}{c} \text{O} \\ \parallel \\ \text{.. N-C-O-} \\ \vdots \\ \text{H} \end{array} + \text{NaH} \longrightarrow \begin{array}{c} \text{O} \\ \parallel \\ \text{.. N-C-O-} \\ \vdots \\ \ominus \end{array} \xrightarrow{\text{Sulfolane}} \begin{array}{c} \text{O} \\ \parallel \\ \text{.. N-C-O-} \\ | \\ \text{CH}_2 \\ | \\ \text{CH}_2 \\ | \\ \text{CH}_2 \\ | \\ \text{SO}_3\text{Na} \end{array}$$

⊖ ⊕

Scheme III. Sulfonation of Urethanes

### Scheme III Sulfonation of Urethanes

-15-

conformational entropy relaxation at the glass transition, which is inversely proportional to the polymer mobility in the rubbery state. In the case of thermoplastic polyurethanes small values of  $\Delta C_p$  to indicate high levels of the physical crosslinking.

Rheovibron dynamic mechanical testing was used to study the dynamic modulus ( $E'$  and  $E''$ ) and internal friction ( $\tan \delta$ ) as a function of temperature and frequency. The dynamic loss modulus, or damping, is sensitive to various molecular motions, structural heterogeneities and morphology of multiphase systems. The largest loss peak, designated as the  $\beta$  peak, is associated with the glass transition temperature. The magnitude of  $\beta$  peak in amorphous polymers is higher than in multiphase polymers, because the chain segments of amorphous polymers are free from the restraints imposed by microphase separation. At a constant degree of phase separation, many small domains are more effective in restraining motion than are a few large domains. The width of the loss modulus peak generally increased as microphase separation increased. The dynamic modulus above  $T_g$  generally increases with increasing degree of microphase separation. This is clearly due to the effect of the physical crosslinking generated by the hard segment polyurethane domains.

The tensile behavior of a strained thermoplastic elastomer generally depends on the size, shape and concentration of the hard domains, intermolecular bonding within the hard domains, and the ability of the soft segments to crystallize under strain.

In this study of the mechanical and thermal properties of segmented polyether polyurethane ionomers, the parameters varied included chain extender type, hard segment content, and degree of ionization. The purpose of this work to investigate how the level of ionization affects morphology and physical properties.

## B. RESULTS AND DISCUSSION

Materials studied in this report are listed in the Table 1. Effects of changes in hard segment content and degree of ammonium sulfonation on the extent of phase separation and related physical properties are summarized in Table 2.

### 1. Differential Scanning Calorimetry

A comparison of thermal characteristics of precursor MDEA chain extended polyether polyurethanes shows that the incorporation of MDEA as chain extender inhibits microphase separation in the segmented polyurethane. This is indicated by the fact that the fraction of hard segments dissolved in the soft phase varies from 0.03 to 0.31. This produces changes in  $T_g$  from  $-54.5^\circ\text{C}$  for sample ET-22-0 to  $-32.0^\circ\text{C}$  for sample ET-37-0. For high MDEA content polymers a wide glass transition zone was observed, suggesting a substantial degree of interphase mixing.

The compatibilization produced by the MDEA is reversed by ammonium sulfonation. Figure 1 shows the effect of ammonium sulfonation on the thermal transitions of selected MDEA chain extended polyether polyurethanes. Similar thermograms were obtained for the other polyurethane zwitterionomers. A progressive

decrease in  $T_g$  and narrowing of the transition zone was observed as the degree of ammonium sulfonation was increased. This suggests that the process of ammonium sulfonation improves the microphase separation and sharpens the interfacial zone between the hard and the soft segment phase. Figure 1 also reveals that the change of heat capacity,  $\Delta C_p$ , at the glass transition decreases with increasing the degree of ammonium sulfonation. This reduction in the entropy of polymer chain segments in the rubbery state is caused by the restraints imposed by the ionically bound hard domains. Mixing of hard segments into the soft phase can also retard the motion of soft segment polymer chains, and cause a decrease in  $\Delta C_p$  as well. However, in comparison with the effect of physical crosslinking resulting from microphase separation, this mixing effect is relatively small.

## 2. Dynamic Mechanical Testing

The dynamic mechanical responses ( $E'$  and  $E''$ ) of MDEA chain extended precursor polyether polyurethane (Table 2) indicates that the incorporation of MDEA inhibits microphase separation. Figure 2 clearly demonstrates how ammonium sulfonation affect the storage and the loss modulus of the ET-37 series zwitterionomers. The storage and the loss modulus of the ET-22, ET-24, and ET-31 series contain similar features and are not shown. The ET-37 series of zwitterionomers shown in Figure 2 exhibits a shift in the  $\beta$  transition to lower temperatures as the degree of sulfonation is increased. This is characteristic of increased microphase separation. Accompanying this improvement in microphase separation

is an increase in the slope of the storage modulus ( $E'$ ) curve at the glass transition, and an enhancement in the rubbery plateau modulus. The modulus enhancement in the rubbery plateau is caused by the hard segment domains which behave as filler particles and act as reinforcement for the soft segment matrix. Coulombic interactions among the ionic sites not only promotes the segregation of hard segments, but also markedly enhances domain cohesiveness. Therefore, the softening point of the hard domains is substantially increased and the rubbery plateau is extended to a higher temperature. For example, ET-37-6.0 maintains a high rubbery plateau modulus of about  $10^8$  N/M<sup>2</sup> up to 170°C, which is unusual for conventional polyurethanes.

### 3. Stress-Strain Testing

The tensile properties of precursor polyether polyurethanes summarized in Table 1 reveal that the Young's modulus (room temperature) increases with increasing hard segment content (MDI-MDEA). This can be accounted for by the fact that the incorporation of MDEA promotes greater phase mixing and tends to raise  $T_g$  close to the test temperature. Figure 3 displays the effect of the variation in the degree of ammonium sulfonation on mechanical properties of the ET-37 series of zwitterionomers. The stress-strain curves for the ET-22, ET-24, and ET-31 series zwitterionomers are similar and are not shown. These materials show a dramatic increase in Young's modulus and ultimate strength with increasing the degree of ammonium sulfonation. The highly sulfonated materials, ET-37-4.8 and ET-37-6.0, exhibit superior tensile properties even though their  $T_g$ s are much lower than that

of their precursor polymer ET-37-0. These observations are explained in terms of sample morphology. The ionic hard segment domains act as the most effective reinforcing filler in these polyurethanes. The stress-strain behavior at high elongation was substantially altered by even small degrees of ammonium sulfonation. These results clearly show the significant impact of even a small level of zwitterionization on the properties of thermoplastic polyurethane elastomers.

### C. SIGNIFICANCE

The introduction of ionic centers into polyurethane elastomers has a profound effect on these material's morphology and physical properties. The importance of ionic interactions has been demonstrated in the studies of MDEA chain extended polyether polyurethane zwitterionomers. The extent of microphase separation, the physical crosslinking effect, ductility, and high temperature properties can be improved or adjusted by ionization of the hard segment. In comparison with commercially available polyether polyurethanes samples such as ET-37-4.8 and ET-37-6.0 show superior tensile strength, and high temperature modulus.

A remarkably unique property of ion containing polymers is their potential solution application via organic or aqueous solvent systems. This unusual feature suggests a wide range of applications, including latex paints or coatings, adhesives, and microporous sheeting materials.

TABLE 1  
MATERIAL CHARACTERIZATION

SAMPLE	MOLAR RATIO			MOLECULAR WEIGHT			WT % SO <sub>3</sub>	
	MDI/MDEA/PTMO			M <sub>n</sub>	M <sub>w</sub>	M <sub>w</sub> /M <sub>n</sub>	CALCULATION*	ELEMENTAL** ANALYSIS
ET-22-0	2	0.25	1.75	6.1×10 <sup>4</sup>	1.5×10 <sup>5</sup>	2.5	0	0
ET-22-0.4	2	0.25	1.75	6.1×10 <sup>4</sup>	1.5×10 <sup>5</sup>	2.5	0.7	0.4
ET-24-0	3	1	2	5.7×10 <sup>4</sup>	1.3×10 <sup>5</sup>	2.3	0	0
ET-24-0.6	3	1	2	5.7×10 <sup>4</sup>	1.3×10 <sup>5</sup>	2.3	0.5	0.6
ET-24-1.2	3	1	2	5.7×10 <sup>4</sup>	1.3×10 <sup>5</sup>	2.3	1.2	1.2
ET-24-1.7	3	1	2	5.7×10 <sup>4</sup>	1.3×10 <sup>5</sup>	2.3	1.9	1.7
ET-30-0	2	1	1	4.1×10 <sup>4</sup>	9.7×10 <sup>4</sup>	2.4	0	0
ET-30-1.5	2	1	1	4.1×10 <sup>4</sup>	9.7×10 <sup>4</sup>	2.4	1.5	1.5
ET-30-2.4	2	1	1	4.1×10 <sup>4</sup>	9.7×10 <sup>4</sup>	2.4	2.4	2.4
ET-30-2.7	2	1	1	4.1×10 <sup>4</sup>	9.7×10 <sup>4</sup>	2.4	3.2	2.7
ET-30-3.9	2	1	1	4.1×10 <sup>4</sup>	9.7×10 <sup>4</sup>	2.4	4.2	3.9
ET-37-0	3	2	1	4.1×10 <sup>4</sup>	1.1×10 <sup>5</sup>	2.7	0	0
ET-37-2.9	3	2	1	4.1×10 <sup>4</sup>	1.1×10 <sup>5</sup>	2.7	2.9	2.9
ET-37-4.8	3	2	1	4.1×10 <sup>4</sup>	1.1×10 <sup>5</sup>	2.7	4.8	4.8
ET-37-6.0	3	2	1	4.1×10 <sup>4</sup>	1.1×10 <sup>5</sup>	2.7	6.6	6.0

\* wt% SO<sub>3</sub> added during synthesis

\*\* wt% SO<sub>3</sub> measured by Galbraith Laboratories, Inc.



TABLE 11

## PHYSICAL PROPERTIES OF MATERIALS

SAMPLE	DSC		RHEOVIBRON		TENSILE PROPERTIES		
	$T_g$ (°C)	TRANSITION ZONE (°C)	$WT_2$	$\beta_{max}$ (°C)	RUBBERY PLATEAU (°C)	$E_y$ ( $10^7 N/M^2$ )	$E_b$ (%)
ET-20-0	-56.5	-67.0 ~ -44.0		-45	-	-	-
ET-22-0	-54.5	-67.0 ~ -41.0	0.03	-42	-20 ~ 90	0.94	0.88
ET-22-0.4	-56.0	-68.0 ~ -42.0	0.01	-44	-22 ~ 95	0.95	0.99
ET-24-0	-50.0	-62.0 ~ -36.0	0.09	-38	-15 ~ 90	0.64	1.15
ET-24-0.6	-51.5	-63.0 ~ -38.0	0.07	-40	-16 ~ 100	0.73	1.54
ET-24-1.2	-53.0	-64.0 ~ -40.0	0.05	-41	-17 ~ 110	0.69	2.59
ET-24-1.7	-55.0	-65.0 ~ -42.0	0.02	-43	-18 ~ 115	0.06	5.01
ET-30-0	-42.0	-62.0 ~ -23.0	0.20	-31	0 ~ 115	1.00	7.70
ET-30-1.5	-46.0	-66.0 ~ -28.0	0.14	-35	-2 ~ 135	1.00	23.10
ET-30-2.4	-49.0	-69.0 ~ -32.0	0.10	-38	-4 ~ 140	1.40	30.10
ET-30-2.7	-51.0	-71.0 ~ -35.0	0.08	-40	-5 ~ 143	1.60	37.10
ET-30-3.9	-55.0	-73.0 ~ -40.0	0.02	-43	-7 ~ 148	2.10	45.50
ET-37-0	-32.0	-65.0 ~ -3.0	0.31	-17	30 ~ 92	2.30	0.35
ET-37-2.9	-41.0	-69.0 ~ -13.0	0.21	-27	25 ~ 145	4.00	42.70
ET-37-4.8	-47.0	-73.0 ~ -23.0	0.13	-33	18 ~ 165	7.80	52.50
ET-37-6.0	-52.0	-76.0 ~ -31	0.06	-40	10 ~ 172	11.40	63.70

\* $WT_2$  is the fraction of hard segment (MDI-MDEA) dissolved in the soft segment phase (MDI-PTMO), calculated using the Gordon Taylor equation:  $T_g = T_{g1} + KWT_2(T_{g2}-T_g)/(1-WT_2)$ ,  $K = 0.62$ ,  $T_{g1}$  and  $T_{g2}$  are -56.5 °C and 54.0 °C respectively.

# DSC CURVES OF POLYURETHANE ZWITTERIONOMERS

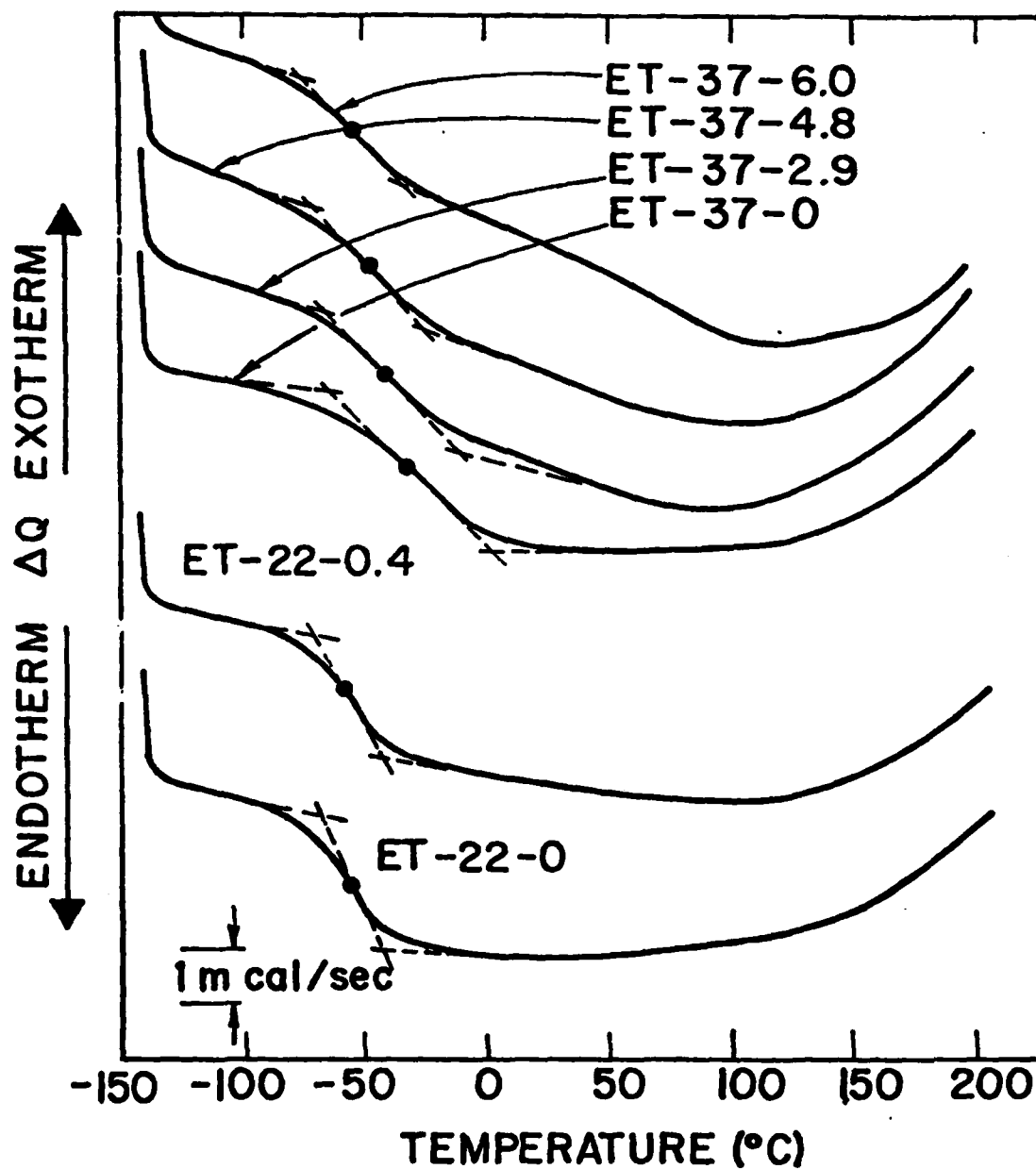


FIG. 1

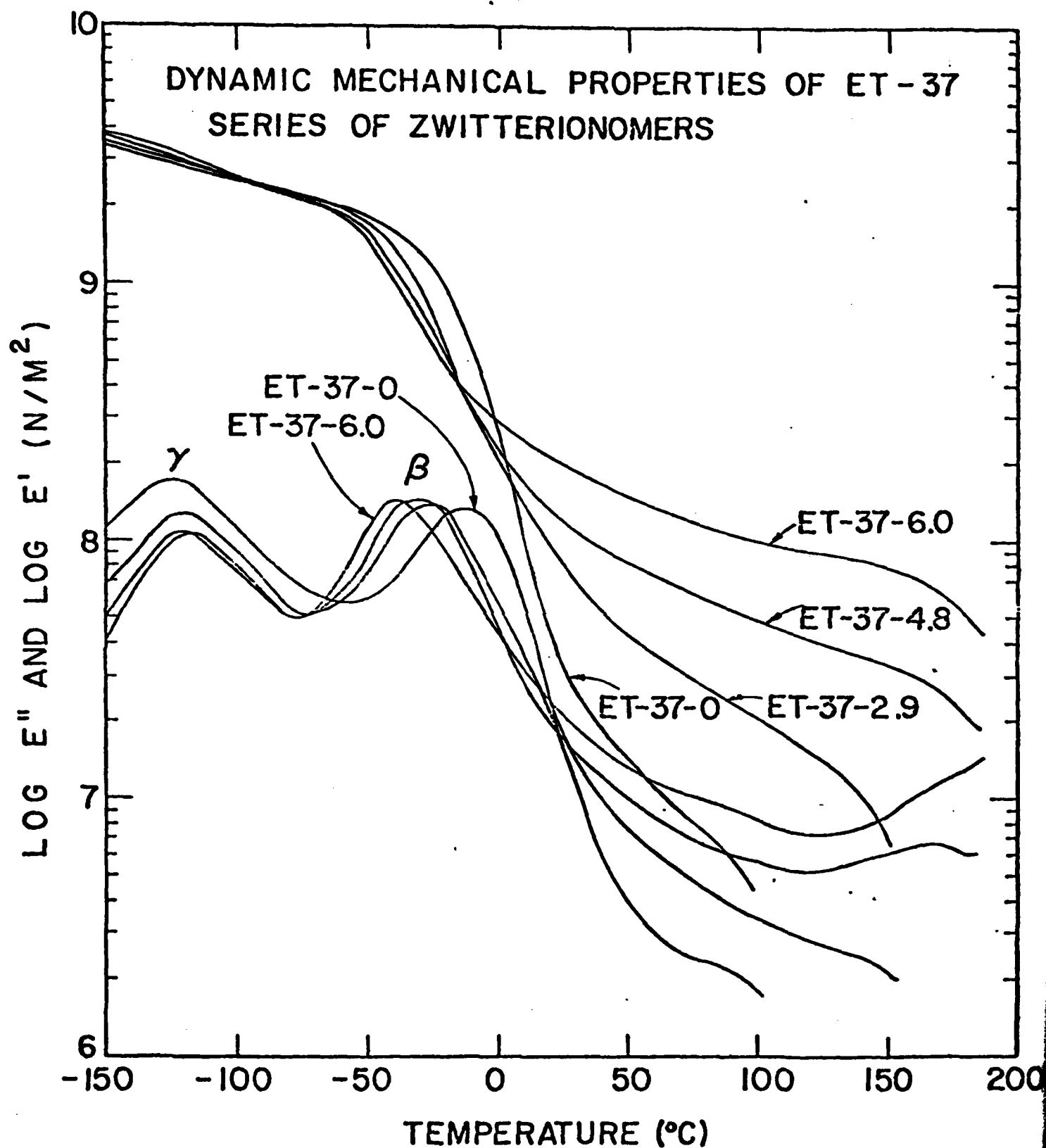


FIG. 2

# STRESS-STRAIN CURVES FOR ET-37 ZWITTER IONOMERS

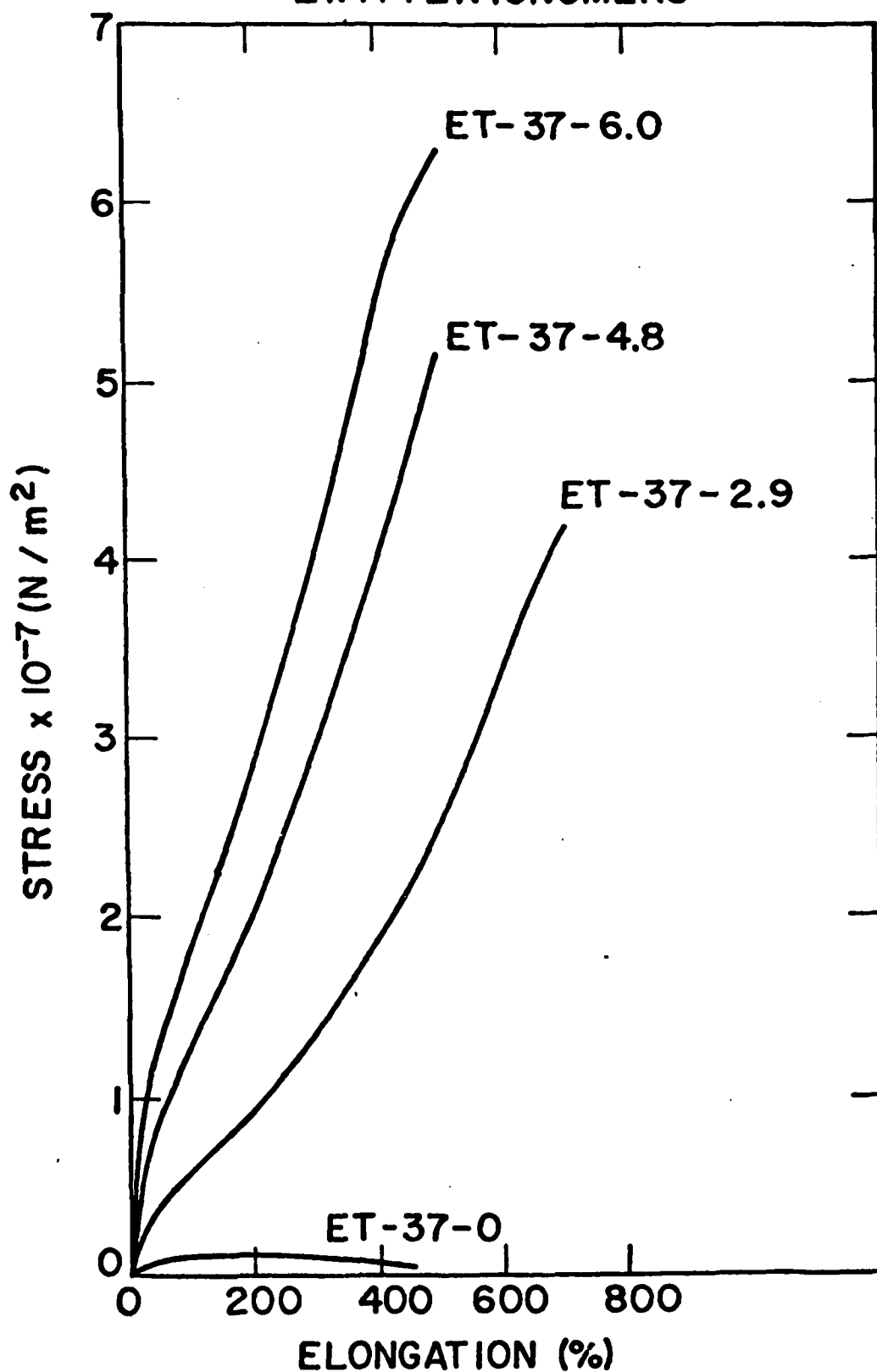


FIG. 3

### III. U.V. CURABLE POLYURETHANES

#### A. INTRODUCTION

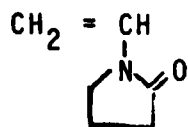
High intensity radiation, from electron beams or ultraviolet sources, has been shown to be an effective means to initiate polymerization in reactive urethane oligomer systems. The advantages of this technology include high throughput, savings in energy, and reduced or eliminated solvent emissions compared to the solvent based systems, since most formulations are 100% reactive oligometric liquids. In general, the system employs a reactive mixture of urethane oligomers tipped with acrylic functionality, combined with vinyl monomers which are added to make harder products and/or to reduce the viscosity of the precursor liquid to obtain better processibility.

The most important component of a flexible and UV curable system in determining the ultimate physical properties in the reactive urethane oligomer. The oligomer usually consists of a diisocyanate such as toluene diisocyanate (TDI) or isophorone diisocyanate (IPDI) tipped with 2-hydroxyethylacrylate (HEA) as a hard segment, and a polyester or polyether soft segment.

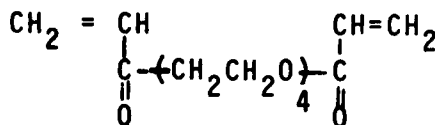
As has been suggested by the studies on urethane block copolymers, the physical properties of UV curable urethane acrylates should depend on the compositions and the morphology of the materials. Only recently, however, have any publications appeared describing the physical properties in any detail.

This systematic study focused on the structure-property relationships of UV curable urethane acrylate systems. The materials considered in this study were TDI and IPDI based urethane acrylates with polycaprolactone diol (PCL) and polytetramethyleneoxide (PTMO)

-27-



NVP



PEGDA

The composition of the UV curable urethane acrylate systems was varied in two ways. First, the molecular weight of soft segment polyol was varied while the crosslinker content was kept constant. In a second series of experiments, the crosslinker content was varied. In total, three systems comprising 21 samples were studied. A description and a designation code for each material is given in Table I.

## 2. Mechanical property measurements.

The Young's modulus, ultimate tensile strength and ultimate elongation of the materials studied are summarized in Table 2. Higher soft segment molecular weight gives lower Young's modulus and ultimate tensile strength. Increasing the crosslinker content leads to an increase in the Young's modulus and ultimate tensile strength. However, the ultimate elongation of I-ET650 decreases with NVP content while that of I-ET2000, T-ET1000, and T-ET2000 increases with NVP. Furthermore increasing NVP content in T-ET2000 materials improved the toughness, while PEGDA did not affect it.

Fig. 1 shows the dynamic mechanical properties of I-ET650 with 0; 10 and 15 wt% NVP. Low temperature transitions located at  $-120^\circ\text{C}$  and  $-60^\circ\text{C}$  are attributed to localized motion in PTMO sequences and absorbed water, respectively. A major glass transition peak is observed that possesses a slight shoulder between 0 and  $25^\circ\text{C}$ . The presence of a single glass transition peak implies that for the most part the I-ET650 series of polymers have a one

phase morphology.

Increasing the NVP content leads to a shift of the major transition peak of the one phase materials to higher temperatures. A crosslinking effect is clearly seen by the slight increase in modulus in the rubbery region and a decrease in  $\tan \delta$  minimum above the glass transition temperature. The increase in crosslink density and glass transition accounts for the tendency of these one-phase materials to become less ductile and more brittle at higher levels of NVP incorporation.

Fig. 2 shows the dynamic mechanical properties of the T-ET2000 series of the materials. The same tendencies were observed in T-ET2000 and T-ET1000 series. These polymers contain two glass transitions which are indicative of a phase separated polymer system. With increasing NVP content, the soft segment glass transition peak at about  $-50^{\circ}\text{C}$  decreases in magnitude without changing position. Good phase separation is obtained despite the fact that the system is crosslinked. Increasing the NVP content leads a shift of hard segment domain glass transition to higher temperatures with an increase in its magnitude. However, PEGDA does not affect the position of the hard segment domain glass transition. This difference was accounted for by the  $T_g$  contribution of NVP and PEGDA in the hard segment domains.

Fig. 3 shows the effects of soft segment molecular weight on mechanical properties of I-ES series of materials. This system exhibits better phase separation as the molecular weight of PCL is increased from 530 to 2000. The same observation was made in the I-ET series of the materials.



### 3. Thermal Analysis

Glass transitions and the endotherm temperatures for each sample were obtained by differential scanning calorimetry and are listed in Table III. The glass transition temperatures of one phase materials and the hard segment glass transition of some of the two phase materials were not observable.

Comparison of the low temperature DSC glass transition to the position of the low temperature glass transition of the dynamic mechanical measurements shows good correspondence. The small, broad high temperature endotherm peak located at about 125°C suggests the existence of short-range ordering associated with urethane linkages in the hard segment domains.

#### C. SIGNIFICANCE

A systematic study of the structure-property relationships in a variety of UV curable acrylates has been accomplished using stress-strain, dynamic mechanical measurements, and differential scanning calorimetry.

The urethane acrylates have a wide range of applications from printing plates to coating materials because of their UV curing characteristics, their flexibility, and abrasion resistance. Thus control of the physical properties of urethane acrylate becomes important in order to obtain suitable properties for a certain application. The present systematic study shows the possibility for material design. The morphology of the materials can be controlled by changing the molecular weight of the soft segment polyols. Young's modulus and ultimate tensile strength can be achieved by incorporation of certain crosslinkers. The

glass transition temperature also depends on the amount and glass transition temperature of the crosslinker used. High ultimate elongation is achieved by promoting microphase separation.

Table I. SAMPLE CHARACTERIZATION

<u>Sample</u>	<u>System Type</u>	<u>Crosslinker</u>	<u>Weight %<sup>*1</sup></u> <u>Hard Segment</u>	<u>Soft Segment</u> <u>Molecular Weight</u>
I-ET650-0	HEA/IPDI/PTMO	None	51.6	650
I-ET650-10N	HEA/IPDI/PTMO	10 wt% NVP	46.4	650
I-ET650-25N	HEA/IPDI/PTMO	25 wt% NVP	38.7	650
I-ET1000-10N	HEA/IPDI/PTMO	10 wt% NVP	40.9	1000
I-ET2000-0	HEA/IPDI/PTMO	None	25.7	2000
I-ET2000-10N	HEA/IPDI/PTMO	10 wt% NVP	23.1	2000
I-ET2000-25N	HEA/IPDI/PTMO	25 wt% NVP	19.3	2000
I-ES530-10N	HEA/IPDI/PCL	10 wt% NVP	50.6	530
I-ES830-10N	HEA/IPDI/PCL	10 wt% NVP	40.9	830
I-ES1250-10N	HEA/IPDI/PCL	10 wt% NVP	36.8	1250
I-ES2000-10N	HEA/IPDI/PCL	10 wt% NVP	23.1	2000
T-ET1000-0	HEA/TDI/PTMO	None	33.8	1000
T-ET1000-10N	HEA/TDI/PTMO	10 wt% NVP	30.4	1000
T-ET1000-25N	HEA/TDI/PTMO	25 wt% NVP	25.3	1000
T-ET1000-10D	HEA/TDI/PTMO	10 wt% PEGDA	30.4	1000
T-ET1000-25D	HEA/TDI/PTMO	25 wt% PEGDA	25.3	1000
T-ET2000-0	HEA/TDI/PTMO	None	23.0	2000
T-ET2000-10N	HEA/TDI/PTMO	10 wt% NVP	20.7	2000
T-ET2000-25N	HEA/TDI/PTMO	25 wt% NVP	17.3	2000
T-ET2000-10D	HEA/TDI/PTMO	10 wt% PEGDA	20.7	2000
T-ET2000-25D	HEA/TDI/PTMO	25 wt% PEGDA	17.3	2000

\*1 HEA and diisocyanate segment

Table II. TENSILE PROPERTIES OF URETHANE ACRYLATES

<u>Sample</u>	<u>Young's Modulus (N/M<sup>2</sup>)</u>	<u>Ultimate Tensile Strength (N/M<sup>2</sup>)</u>	<u>Ultimate Elongation</u>	<u>Yield Strength (N/M<sup>2</sup>)</u>
I-ET650-0	2.65x10 <sup>7</sup>	1.07x10 <sup>7</sup>	77.1%	-
I-ET650-10N	4.36x10 <sup>8</sup>	2.07x10 <sup>7</sup>	48.3%	-
I-ET650-25N	1.46x10 <sup>9</sup>	4.48x10 <sup>7</sup>	4.6%	-
I-ET1000-10N	4.34x10 <sup>7</sup>	1.29x10 <sup>7</sup>	100.0%	-
I-ET2000-0	3.98x10 <sup>6</sup>	2.14x10 <sup>6</sup>	80.6%	-
I-ET2000-10N	1.29x10 <sup>7</sup>	6.52x10 <sup>6</sup>	96.7%	-
I-ET2000-25N	1.38x10 <sup>8</sup>	1.83x10 <sup>7</sup>	162.5%	-
I-ES530-10N	5.22x10 <sup>8</sup>	2.11x10 <sup>7</sup>	44.2%	1.73x10 <sup>7</sup>
I-ES830-10N	7.99x10 <sup>7</sup>	1.71x10 <sup>7</sup>	100.2%	-
I-ES1250-10N	1.54x10 <sup>7</sup>	1.37x10 <sup>7</sup>	126.0%	-
I-ES2000-10N	7.81x10 <sup>6</sup>	7.21x10 <sup>6</sup>	127.0%	-
T-ET1000-0	4.16x10 <sup>7</sup>	1.86x10 <sup>7</sup>	62.2%	-
T-ET1000-10N	1.29x10 <sup>8</sup>	3.18x10 <sup>7</sup>	76.6%	-
T-ET1000-25N	9.04x10 <sup>8</sup>	8.95x10 <sup>7</sup>	78.7%	-
T-ET1000-10D	5.76x10 <sup>7</sup>	2.22x10 <sup>7</sup>	56.3%	-
T-ET1000-25D	9.01x10 <sup>7</sup>	2.42x10 <sup>7</sup>	40.7%	-
T-ET2000-0	5.83x10 <sup>6</sup>	3.84x10 <sup>6</sup>	91.8%	-
T-ET2000-10N	1.92x10 <sup>7</sup>	7.99x10 <sup>6</sup>	112.0%	-
T-ET2000-25N	1.27x10 <sup>8</sup>	2.08x10 <sup>7</sup>	140.0%	-
T-ET2000-10D	1.03x10 <sup>7</sup>	5.48x10 <sup>6</sup>	86.3%	-
T-ET2000-25D	2.33x10 <sup>7</sup>	7.58x10 <sup>6</sup>	58.5%	-

Table III THERMAL PROPERTIES OF URETHANE ACRYLATES, NVP AND PEGDA

Sample	Glass Transition Temperature (°C)				Endotherm Temperature (°C)			
	T <sub>g1</sub>		T <sub>g2</sub>		T <sub>m</sub>			
	Control	Quench	Control	Quench	Control	Quench	Control	Quench
I-ET650-0	-	-	-	-	52.6, 163.0	-	-	-
I-ET1000-10N	-47.6	-43.0	38.8	-	141.0	-	-	-
I-ET2000-0	-73.5	-71.0	-	-	156.0	-	-	-
I-ET2000-10N	-73.0	-71.0	-	-	166.0	-	-	-
I-ET2000-25N	-73.0	-72.0	-	-	-	-	-	-
I-ES530-10N	-	-	-	-	59.0, 147.0	-	-	-
I-ES830-10N	-	-	-	-	159.0	-	-	-
I-ES1250-10N	-46.0	-45.0	-	-	144.6	-	-	-
I-ES2000-10N	-62.0	-55.0	-	-	-	-	-	-
T-ET1000-0	-58.0	-58.0	-	-	128.4	-	-	-
T-ET1000-10N	-60.0	-60.0	39.0	-	132.6	-	-	-
T-ET1000-25N	-58.0	-58.0	40.0	-	134.5	-	-	-
T-ET1000-10D	-56.0	-56.0	-	-	133.8	-	-	-
T-ET1000-25D	-58.0	-62.0	-	-	142.0	-	-	-
T-ET2000-0	-78.0	-84.0	-	-	124.4	-	-	-
T-ET2000-10N	-80.0	-84.0	40.0	-	140.4	-	-	-
T-ET2000-25N	-80.0	-84.0	42.0	-	133.0	-	-	-
T-ET2000-10D	-77.0	-79.0	-	-	138.5	-	-	-
T-ET2000-25D	-80.0	-80.0	-	-	146.0	-	-	-
cured NVP	-	-	73.2	73.2	-	-	-	-
cured PEGDA	-	-	21.0	21.0	-	-	-	-

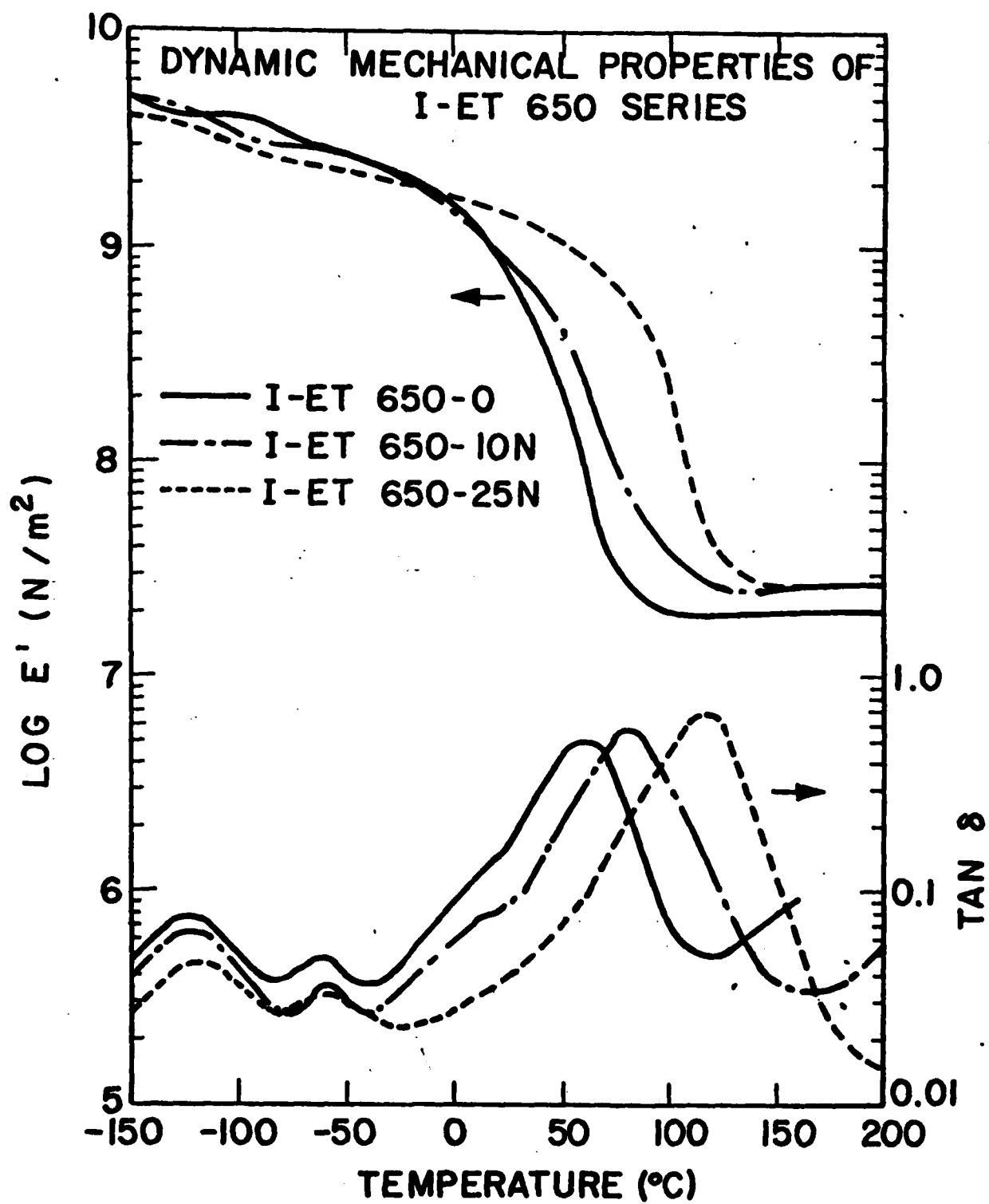


FIG. 1

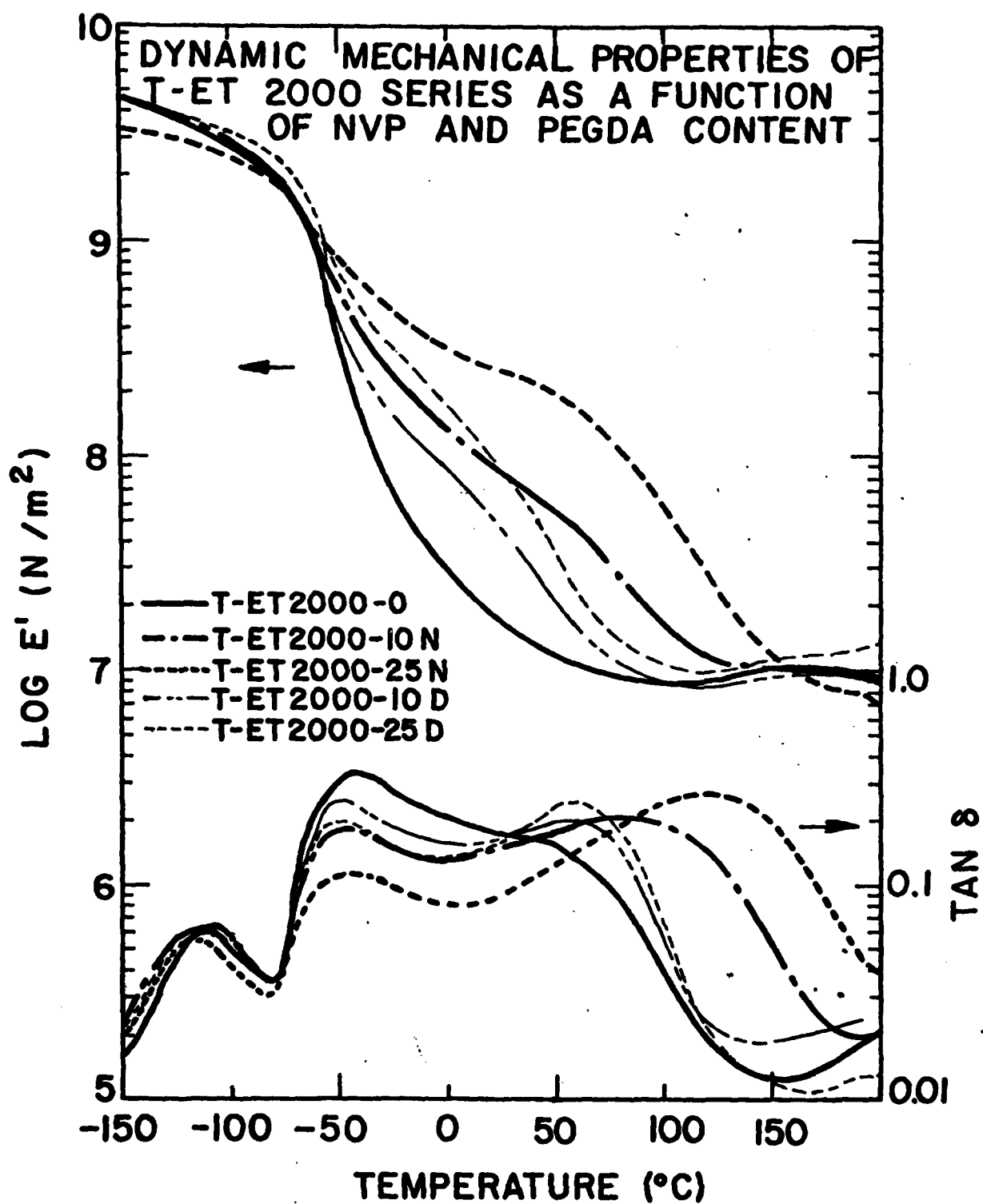


FIG 2

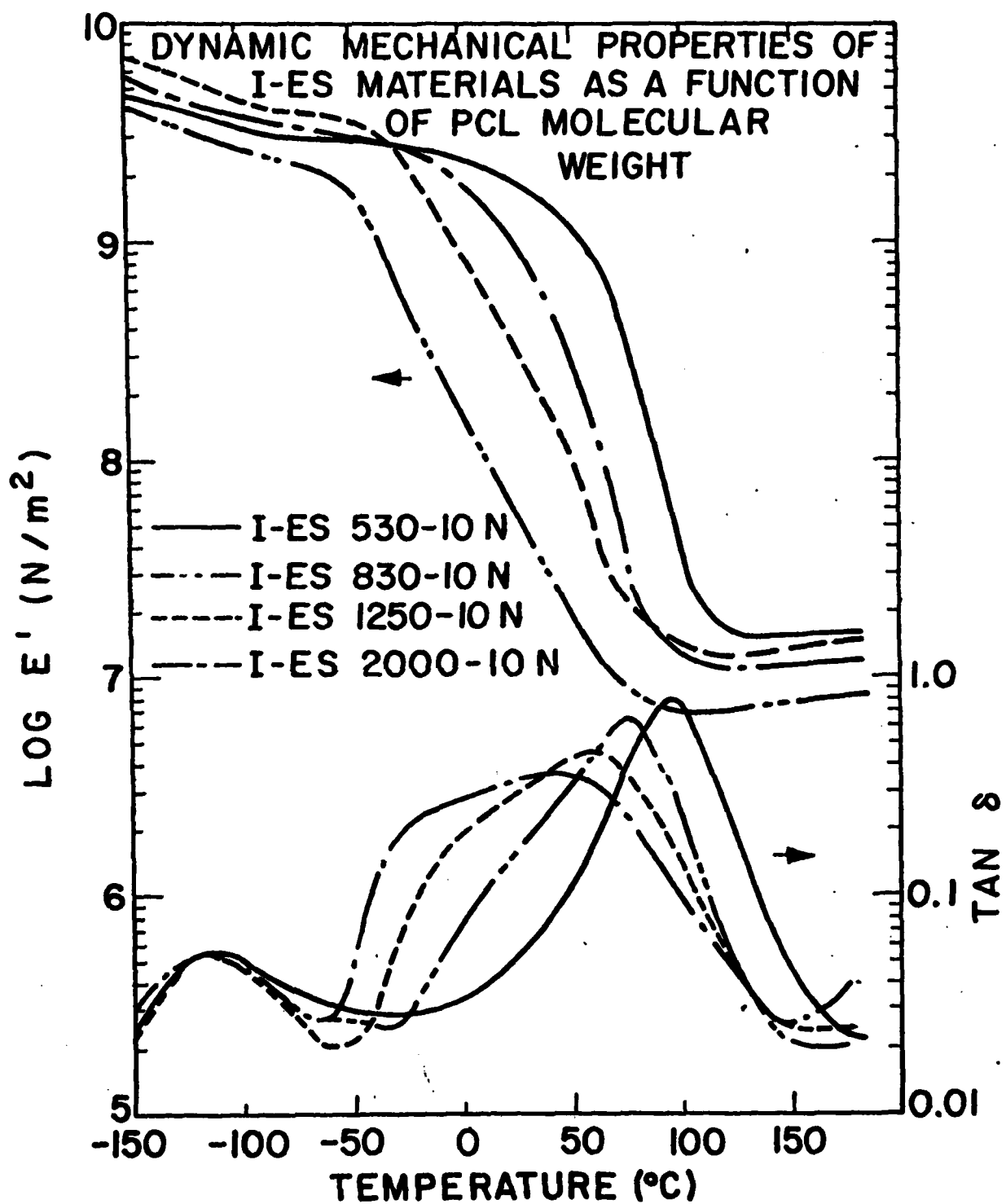


FIG. 3



DISTRIBUTION LIST for Reports

<u>Addressee</u>	<u>Copies</u>
Commander Naval Air Systems Command Dept. of the Navy Washington, DC 20361 ATTN: Code AIR-5163D2	4
Commander Naval Air Systems Command Dept of the Navy Washington, DC 20361 Attn: Code AIR-954	8
Commander Naval Air Systems Command Dept of the Navy Washington, DC 20361 Attn: Code AIR-320A	1
Commander Naval Surface Weapons Center White Oak, Silver Spring, MD 20910 Attn: Dr. Joseph Augl (Code 234)	1
Air Force Materials Laboratory Wright-Patterson AFB, OH 45433 Attn: Codes MBC    MXE LN    LAE LT    LAM	6
Director Plastics Technical Evaluation Center U.S. Army Armanent Research & Development Command Dover, NJ 07801	1
Hercules Incorporated Magna, UT 84044 Attn: Mr. E. C. Crossland	1
TRW One Space Park Redondo Beach, CA 90278 Attn: R. W. Vaughan	1
University of Maryland College Park, MD 20742 Attn: Dr. W. J. Bailey	1
Naval Research Laboratory Washington, DC 20375 Attn: Dr. W. D. Bascom, Chemistry Div. (Code 6170)	1

Distribution List (Continued)

Page 2 of 4

North American Aviation  
Rockwell International  
Columbus Division  
4300 E. Fifth Ave  
Columbus, OH 43216

1

Commanding Officer  
Naval Air Development Center  
Warminster, PA 18974  
Attn: Aero Materials Laboratory (Code 6060)  
(Structures Division)

1

Northrup Corporation  
1001 E. Broadway  
Hawthorne, CA 90250  
Attn: Technical Library

1

Lockheed California Co  
Dept. 74-54, Bldg 63  
Box 551  
Burbank, CA 91503  
Attn: Mr. J. H. Wooley

1

Naval Research Laboratory  
Washington, DC 20350  
Attn: Code 6120 (1 copy)  
Code 8433 (1 copy)

2

The Boeing Co.  
Aerospace Division  
P. O. Box 3707  
Seattle, WA 98124  
Attn: Library

1

Office of Naval Research  
Washington, DC 20361  
Attn: Code 471

1

NASA Headquarters  
609 Independence Ave., S.W.  
Washington, DC 20546  
Attn: Library

1

Battelle  
Columbus Laboratories  
505 King Avenue  
Columbus, OH 43201

1

Commander  
Naval Material Command Hdqtrs  
Washington, DC 20361  
Attn: Code MAT 04H

1

DISTRIBUTION LIST (Cont'd)

Page 3 of 4

Lockheed Missiles and Space Center  
Sunnyvale, CA 94088  
Attn: Mr. Clayton May

1

Materials Engineering Laboratory  
U.S. Army Armament R&D Command  
Dover, NJ 07801  
Attn: Mr. R. F. Wegman

1

National Academy of Science  
2101 Constitution Ave., N.W.  
Washington, DC 20418  
ATTN: Dr. R. S. Shane, NMAA

1

Stanford Research Institute  
333 Ravenswood Ave  
Menlo Park, CA 94025  
Attn: Mr. Milan Maximovich (1 copy)  
Technical Library (1 copy)

2

Commander, Naval Ship Engineering Center  
National Center #2, Room 5E52  
Washington, DC 20361  
Attn: Mr. John Alfors

1

Commanding Officer  
Naval Air Rework Facility  
Naval Air Station  
Norfolk, VA 23511  
Attn: Mr. Harold Sommerflek, Code 343.

1

Commanding Officer  
Naval Air Rework Facility  
Naval Air Station  
Jacksonville, FL 32212  
Attn: Code 343

1

Commanding Officer  
Naval Air Rework Facility  
Marine Corps Air Station  
Cherry Point, NC 28533  
Attn: Mr. Fred Latham, Code 343

1

Commanding Officer  
Naval Air Rework Facility  
Naval Air Station  
North Island, San Diego, CA 92123  
Attn: Ms Carol Duesler, Code 343

Commanding Officer  
Naval Air Rework Facility  
Naval Air Station  
Alameda, CA 94501  
Attn: Mr. Norman Andur, Code 343

1

DISTRIBUTION LIST (Contd)

Page 4 of 4

Commanding Officer  
Naval Air Rework Facility  
Naval Air Station  
Pensacola, FL 32508  
Attn: Mr. Faoro, Code 343

1

McDonnell Douglas Airplane Co  
P. O. Box 516  
St. Louis, MO 63166  
Attn: Dr. James Carpenter (Materials)

1

Grumman Aerospace Corp.  
Bethpage, NY 11714  
Attn: Technical Library

1

DATE  
FILMED  
8